ChemPubSoc Europe

DOI: 10.1002/cssc.201501128

CHEMSUSCHEM Full Papers

High-Performing Polycarbazole Derivatives for Efficient Solution-Processing of Organic Solar Cells in Air

Ignasi Burgués-Ceballos,*[a] Felix Hermerschmidt,[a] Alexander V. Akkuratov,[b] Diana K. Susarova,[b] Pavel A. Troshin,[b] and Stelios A. Choulis[a]

The application of conjugated materials in organic photovoltaics (OPVs) is usually demonstrated in lab-scale spin-coated devices that are processed under controlled inert conditions. Although this is a necessary step to prove high efficiency, testing of promising materials in air should be done in the early stages of research to validate their real potential for low-cost, solution-processed, and large-scale OPVs. Also relevant for approaching commercialization needs is the use of printing techniques that are compatible with upscaling. Here, solution processing of organic solar cells based on three new poly(2,7-carbazole) derivatives is efficiently transferred, without significant losses, to air conditions and to several deposition methods using a simple device architecture. High efficiencies in the range between 5.0% and 6.3% are obtained in (rigid) spin-coated, doctor-bladed, and (flexible) slot-die-coated devices, which surpass the reference devices based on poly[*N*-9′-heptadecanyl-2,7-carbazole-*alt*-5,5-(4′,7′-di-2-thienyl-2′,1′,3′-benzothiadiazole)] (PCDTBT). In contrast, inkjet printing does not provide reliable results with the presented polymers, which is attributed to their high molecular weight. When the device area in the best-performing system is increased from 9 mm^2 to 0.7 cm^2, the efficiency drops from 6.2% to 5.0%. Photocurrent mapping reveals inhomogeneous current generation derived from changes in the thickness of the active layer.

Introduction

Progress in organic photovoltaics (OPVs) has been largely linked to the development of materials for the active layer, typically based on highly conjugated systems.[1] Lowering the energy bandgap is known to be beneficial for maximizing the amount of harvested photons, thus increasing photocurrent generation. On the other hand, the delivered voltage is related to the energy of those photons; thus, an optimum compromise is thought to be achieved at an energy bandgap of about 1.45 eV.[2] In the bulk heterojunction approach,[3] the incorporation of alternating electron donor–acceptor units in the molecule backbone, either in small molecules[4] or in polymers,[5] is currently widely implemented to enhance charge transport properties.[6] High molecular weight additionally enhances carrier mobility and might lead to a better device performance owing to the reduced hopping distances within the active layer.[7] Other interesting approaches include tuning solubility properties by changing the nature of side chains and substituents,[8] which in turn can also affect charge mobility.[9] All these developments undoubtedly contribute to the increase of efficiency in OPV devices.

High-performing materials are, however, often only demonstrated in small-scale devices, which have been processed under inert conditions using spin coating, a technique which is not compatible with large-scale processes. In some illustrative cases, considerable scientific effort went into OPV systems based on promising materials that were later demonstrated to be inherently degraded upon exposure to air and light.[10] On the other hand, amongst the reported high-performing materials, poly[*N*-9′-heptadecanyl-2,7-carbazole-*alt*-5,5-(4′,7′-di-2-thienyl-2′,1′,3′-benzothiadiazole)] (PCDTBT)[11] has been proven to show high stability in air.[12] As an example, OPV devices based on PCDTBT have been successfully prepared by spray coating in air.[13] It is, therefore, desirable to demonstrate high performances in air using upscalable techniques, ideally in the early stages of research, to quickly scan which materials might be potentially relevant for industrial OPV fabrication. In this work, we propose a simple methodology to address this objective.

Herein, three new high-molecular-weight low-bandgap polymers containing carbazole, benzothiadiazole, and thiophene units with different alkyl side chains are tested in normal structured OPV devices under the referred conditions and premises. Spin coating is used both in inert conditions and in air to build reference devices that are compared to those processed in air using doctor blading, inkjet printing, and slot-die coating. The latter provides a stronger argument for high-throughput processing such as roll-to-roll as it is shown on flexible substrates. Finally, initial steps on the upscaling of the device area are pre-

[a] *Dr. I. Burgués-Ceballos, Dr. F. Hermerschmidt, Prof. S. A. Choulis*
Molecular Electronics and Photonics Research Unit
Department of Mechanical Engineering and Materials Science and Engineering
Cyprus University of Technology
45 Kitiou Kyprianou Street, Limassol, 3041 Cyprus
E-mail: ignasi.burgues@cut.ac.cy

[b] *Dr. A. V. Akkuratov, Dr. D. K. Susarova, Dr. P. A. Troshin*
Institute for Problems of Chemical Physics
Russian Academy of Sciences
Semenov Prospect 1, Chernogolovka, Moscow region 142432 (Russia)

Supporting Information for this article is available on the WWW under http://dx.doi.org/10.1002/cssc.201501128.

sented and discussed. Despite the results still being achieved under lab conditions and on relatively small scales, we hope that this perspective will contribute to stimulating and accelerating research on new photoactive materials for OPV towards industrial needs. This vision is shared by an increasing number of groups worldwide according to recent publications.[14]

Results and Discussion

Conjugated polymers

We recently developed a family of conjugated polymers comprising an extended TTBTBTT building block as compared to the widely used TBT unit (T—thiophene, B—benzothiadiazole).[15] In particular, a carbazole-based copolymer P1 (Figure 1), which can be defined as PCDTTBTBTT in the same way as PCDTBT, showed advanced optoelectronic properties such as a narrow band gap of 1.65 eV and a deep-lying HOMO energy level (−5.44 eV), thus enabling generation of appreciably high current densities in combination with good open circuit voltages (V_{oc}) in solar cells.[15] Here, we also present a polymer P2 that differs from P1 by longer alkyl substituents at the carbazole ring (C_8 in P1 is replaced with C_{10} in P2, Figure 1). The synthesis of this polymer was performed following a general approach presented for P1 previously.[15] Briefly, a Suzuki–Miyamura polycondensation reaction involving corresponding carbazole-based diboronic acid ester and BrTTBTBTTBr monomers yielded the target polymer P2 in high molecular weights: weight average molecular weight $M_w \approx 203$ kDa, polydispersity index PDI ≈ 4.6 (see details of the synthesis in Experimental Section).

We also recently reported a statistical carbazole–fluorene–TTBTBTT terpolymer P3.[15] This material has a low HOMO energy (−5.56 eV) owing to the presence of the fluorene units in its molecular structure, which led to enhanced V_{oc} and solar cell power conversion efficiencies compared to the "pure" carbazole-based analog P1.

The optoelectronic properties of the designed polymers P1–P3 strongly suggest that they are capable of delivering high efficiencies in organic bulk heterojunction solar cells. Thus, according to the theoretical model proposed by Scharber and co-workers,[2] the single-junction devices based on blends of P1–P3 with the acceptor [6,6]-phenyl-C_{71}-butyric acid methyl ester ($PC_{70}BM$) have ultimate efficiencies of 9–11%. Moreover, this family of materials demonstrated excellent photochemical, thermal, and operational stability in pristine thin films and completed photovoltaic devices.[15] These results emphasize the need for further investigation of polymers P1–P3 as promising photoactive materials for large-area solution-processed organic photovoltaics.

Processing of OPVs in air

A series of OPV devices based on conjugated polymers of P1–P3 and PCDTBT were fabricated using the same standard structure, with the only difference being the deposition method used for the active layer. In all cases the active layer consisted of a blend of the electron donor polymer and the electron acceptor $PC_{70}BM$. The resulting current density–voltage (*J–V*) characteristics, and the performance parameters are shown in Figure 2 and Table 1. The solar cell efficiencies obtained using polymers P1–P3 range from 5.0% to 6.3%. These efficiencies represent a significant improvement in comparison with the reference PCDTBT, where measured efficiencies were between 3.9% and 4.7%. Note that these values could be potentially increased by using higher-molecular-weight PCDTBT and by changing the cast solvent.[7,16] Interestingly, only minor variations were observed when moving from inert conditions to air and from spin coating to upscalable techniques such as doctor blading or slot-die coating. This consistency in the performance regardless of the deposition method and conditions proves the stability of these high-performing polycarbazole derivatives during processing and is potentially a solid argument for upscaling. In our opinion, reaching this important milestone, either in standard or in inverted structure, would now

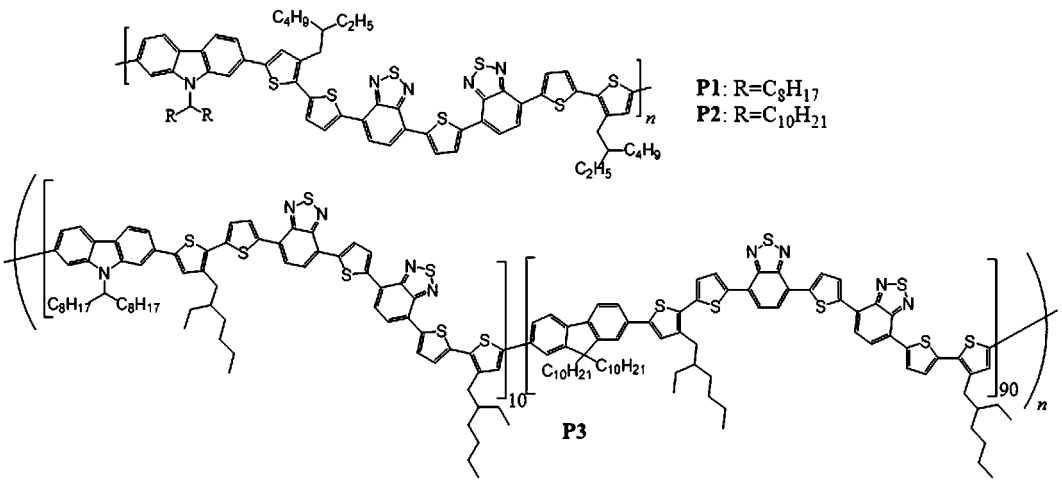

Figure 1. Molecular structures of polymers P1–P3.

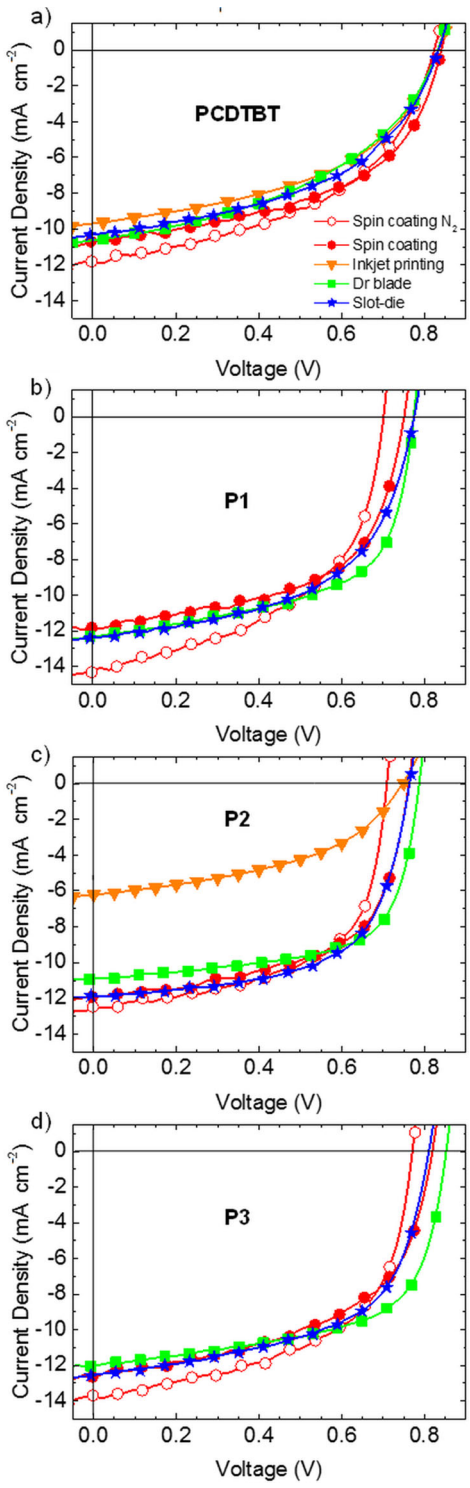

Figure 2. *J–V* characteristics of OPV devices based on different donor polymers PCDTBT (a), P1 (b), P2 (c), P3 (d), with the active layer being processed using spin coating under inert conditions (empty circles) or in air (filled circles), inkjet printing (triangles), doctor blade (squares), or slot-die coating (stars).

justify further research to increase the OPV performance, for example, through interface engineering.[17]

The obtained data reveals a general trend that spin coating under inert conditions results in a slightly higher photocurrent (presented as short-circuit current density, J_{sc}) and slightly lower V_{oc}. This observation is in agreement with other works, where a small increase in V_{oc} upon processing in air has been assigned to the hydration of the poly(3,4-ethylenedioxythiophene):poly(styrenesulfonate) (PEDOT:PSS) hole-extraction layer, resulting in an increase in its work function.[18] On the other hand, the decrease in J_{sc} could be explained in terms of a reduction in charge-carrier mobility, possibly resulting from the generation of trap states upon exposure to air and light.[19] However, deposition of the photoactive layers under ambient conditions does not lead to any significant losses in the fill factor (FF). Another trend observed in the three new polymers is that, when processed in air, the doctor blade technique provides higher power conversion efficiency (PCE) and FF than slot-die coating, which in turn appears to work better than spin coating. A slightly smoother layer and subsequent enhanced interface contact could be one reason for these small improvements when using the doctor blade. Another reason could be related to morphological differences within the bulk heterojunction layer owing to the dissimilar drying kinetics of the coating methods used. However, we believe that such differences were minimized by 1) applying high temperature to the substrate during doctor blading (95 °C) and slot-die coating (70 °C) and 2) subjecting the samples to a post-annealing treatment. Still, the results achieved on flexible devices using slot-die coating are promising: efficiencies surpass 90–95% of the rigid doctor blade counterparts and an even slightly higher photocurrent is generated. The lower V_{oc}, once again, could be ascribed to a poorer interface contact with the cathode due to a rougher topography.[20]

Table 1. Summary of polymer properties and OPV performance parameters as a function of the deposition method used for the active layer. NA: not available.

Polymer	M_w [g mol^{-1}]	PDI	Deposition method[a]	V_{oc} [mV]	J_{sc} [mA cm^{-2}]	FF [%]	PCE [%]
PCDTBT	~16k	2.0	SC (N_2)	824	11.82	48.8	4.75
			SC	842	10.70	52.2	4.70
			IJP[b]	834	9.70	47.8	3.86
			DB[b]	833	10.60	44.1	3.89
			SD	834	10.34	48.3	4.17
P1	~190k	6.3	SC (N_2)	702	14.23	50.9	5.08
			SC	752	11.87	56.4	5.03
			IJP	NA	NA	NA	NA
			DB	775	12.30	59.8	5.70
			SD	776	12.40	57.5	5.53
P2	~203k	4.6	SC (N_2)	709	12.53	59.8	5.31
			SC	764	11.92	59.3	5.40
			IJP	747	6.21	45.5	2.11
			DB	786	10.92	65.8	5.65
			SD	764	11.86	61.7	5.59
P3	~299k	5.3	SC (N_2)	771	13.74	55.5	5.88
			SC	819	12.58	52.8	5.44
			IJP	NA	NA	NA	NA
			DB	852	12.03	61.6	6.31
			SD	811	12.56	57.2	5.83

[a] SC = spin coating, IJP = inkjet printing, DB = doctor blading, SD = slot-die coating. [b] Taken from our previously reported work.[21]

The surprisingly low or unaffordable results obtained using inkjet printing deserve a special discussion. Taking as a reference our previously reported results for PCDTBT, where efficiencies obtained using inkjet printing were comparable to that provided by the doctor blade technique,[21] one could expect similar results for the new series of the carbazole-based copolymers P1–P3. However, we experienced serious technical difficulties to achieve reliable jetting of the inks. Although all solutions were filtered prior to cartridge loading, nozzle clogging occurred in a short time. This phenomenon has been described in previous studies and is known to be sensitive to the molecular weight and gelation dynamics of the printed polymers.[22] As shown in Table 1, the molecular weights of the new polymers are more than ten times larger than that of PCDTBT. In fact, using P3, which is the polymer with the highest molecular weight, no jetting was achieved at all. On the other hand, nozzle clogging was observed when using P1-based solution in less than 10 min after cartridge loading, which is insufficient for reliable printing. Finally, several layers could be printed from a P2-based solution by carefully tuning key printing parameters such as cartridge temperature, piezoelectric waveform, and firing voltage. Even so, more than a twofold decrease in efficiency was obtained in comparison with other applied deposition techniques (see Figure 2c). Despite the fact that the active layer thickness was adjusted to the target 80 nm by varying the drop spacing, the inkjet-printed devices gave rise to much lower FF and J_{sc}. These observations suggest that the morphology of the inkjet-printed layers is likely far from being optimal. The lower drying kinetics associated with inkjet printing[23] might be partially responsible for such large differences as they can induce important changes in the blend morphology. The fact that nozzle clogging was faster in P1 than in P2, even though the molecular weight of P1 is lower, might be related to the lower solubility of P1 and the subsequent faster gelation. These results clearly indicate that inkjet printing is a more restrictive technique for depositing layers of high-molecular-weight polymers than doctor blading or slot-die coating. Possibly specific technical requirements such as larger nozzle diameter and higher firing voltage could be considered. Alternatively, higher PCE inkjet-printed devices could be achieved by modifying material and/or ink properties to fulfil relevant inkjet printing conditions.[21]

Increasing the cell area

It is well known that enlarging the active area of an OPV device results in a significant decrease in overall efficiency, often observed as a simultaneous drop in J_{sc}, FF, and V_{oc}.[24] This has been attributed to inhomogeneities across the active layer and also to the losses due to a relatively high electrode sheet resistance.[25]

As a second step in our strategy, we propose to increase moderately the active area of the device while keeping substrate dimensions and processing conditions the same. We believe that moving from the mm^2 to the cm^2 scale can be useful in many cases to detect resulting defects in the active layer while the impact of electrode sheet resistance would still be negligible. In this work, we compared a series of devices with active areas of 9 mm^2 and 0.7 cm^2. Then, we combined standard *J–V* characterization under simulated sunlight with light-beam-induced current (LBIC) to examine possible losses related to the current generation. For this purpose, a 0.7 cm^2 OPV device based on polymer P3 was prepared using doctor-blade coating as this system led to the highest PCE from the entire set of 9 mm^2 samples. The resulting *J–V* characteristics depicted in Figure 3 reveal, not surprisingly, a simultaneous decrease in V_{oc}, J_{sc}, and FF (see also Table 2). However, the 5.02% PCE of the 0.7 cm^2 OPV cell is still higher than 80% of the PCE of the device with the smaller area.

LBIC analysis (see Figure 4) provides interesting insights into the origin of photocurrent losses. Although a highly homogeneous current distribution is observed in the small device across the whole active area (Figure 4a), the larger device shows inefficient current generation in the upper region (Figure 4b). In particular, we observed the appearance of a gradient of photocurrent in several devices. Since the same gradients but in inverted symmetry were obtained when the measure-

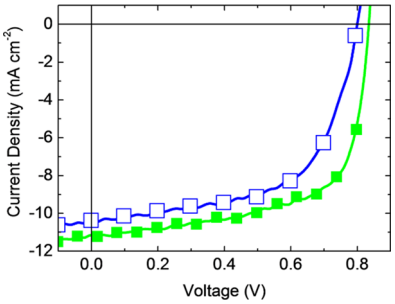

Figure 3. *J–V* characteristics of doctor bladed devices based on polymer P3 with 9 mm^2 (full squares) and 0.7 cm^2 (empty squares) active area.

Table 2. Performance parameters of doctor-bladed devices based on polymer P3.

Device area [mm^2]	V_{oc} [mV]	J_{sc} [mA cm^{-2}]	FF [%]	PCE [%]
9	836	11.22	65.7	6.16
70	800	10.39	60.4	5.02

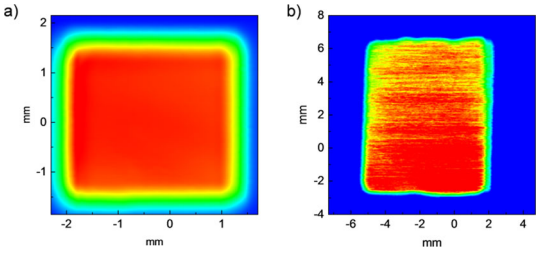

Figure 4. Photocurrent maps of a) 9 mm^2 and b) 0.7 cm^2 OPV devices based on polymer P3 and prepared by doctor-blade coating. The measurements were performed using a mask to define the exact active area.[26]

ments were repeated on the same samples rotated by 180°, contributions to losses related to charge collection caused by the measurement itself can be neglected. We, therefore, ascribe this gradient in photocurrent to a small gradient in thickness derived from the coating process. It has been demonstrated that the performance of PCDTBT-based devices is highly sensitive to the thickness of the active layer[27] to which J_{sc} is related to a great extent. In the process of optimizing the processing conditions of this set of polymers, we also observed critical changes in J_{sc} with small variations in thickness. In doctor-blade coating a small tilt angle of the substrate is enough to create a gradient in thickness. Although the overall efficiency was not greatly decreased when enlarging the cell area from the mm^2 to the cm^2 scale, these data point to the active layer being responsible for this moderate decrease. The LBIC analysis is a useful technique to elucidate possible reasons for decreases in J_{sc}. In the case of the polycarbazole derivative P3, a critical influence of the active layer thickness on the current generation is shown.

In summary, we have presented a new set of polycarbazole derivatives for OPVs that can be processed under air conditions using different coating techniques, including industrially compatible methods. Similar device performances are obtained compared to inert processing, which validate the robustness of these functional materials. Yet on a lab scale, when moving from mm^2 to cm^2 device area, we have identified initial defects in photocurrent generation deriving from the formation of an inhomogeneous active layer. This suggests that including the cm^2 scale in lab research can provide useful initial information related to upscaling challenges. Upscaling processes demand large-area-device and module fabrication combined with low-cost electrodes.[28] Such studies will be of high relevance for this interesting class of materials, which combine several key requirements related to product development targets.

Conclusions

It is of critical importance that new high performing materials for organic photovoltaics (OPVs) demonstrate stability upon processing in air while still giving rise to high efficiencies. A set of new carbazole-based copolymers have been tested in OPV devices, which have shown no significant losses in overall efficiency when processed in air, thereby proving their robustness and suitability for upscaling. Amongst the techniques used, doctor blading has resulted in the highest efficiencies (between 5.7% and 6.3%). Slot-die coating on flexible substrates has also led to high efficiencies above 5.5%. In contrast, inkjet printing has been unsuccessful because of rapid nozzle clogging as a consequence of the high molecular weight of the polymers. Only polymer P2, with higher solubility and longer gelation time, has shown reliable jettability although lower efficiencies have been obtained. Enlarging the cell area of the best-performing system from 9 mm^2 to 0.7 cm^2 has resulted in a moderate decrease of the performance, partially due to inhomogeneous current generation. A critical impact of the active layer thickness on the photocurrent has been deduced. The high OPV performance of the carbazole-based copolymers presented indicates the potential of this class of materials for OPV upscaling requirements.

Experimental Section

Synthesis of conjugated polymers P1–P3

The synthesis and characterization of the polymers P1 ($M_w = 190$k, PDI = 6.3) and P3 ($M_w = 299$k, PDI = 5.3) was reported previously in Ref. [15].

A new polymer P2 was synthesized as follows. The corresponding monomers 9-(henicosan-11-yl)-2,7-bis(4,4,5,5-tetramethyl-1,3,2-dioxaborolan-2-yl)-9*H*-carbazole (713.7 mg, 1.0 mmol) and 2,5-bis{7-[5′-bromo-3′-(2-ethylhexyl)-(2,2′-bithiophen)-5-yl]benzo[c][1,2,5]thiadiazol-4-yl}thiophene (1063 mg, 1.0 mmol) were introduced into a 50 mL round-bottom three-necked flask equipped with a thermometer and a reflux condenser. Toluene (25 mL), 2 M aqueous K_2CO_3 solution (2 mL), aliquat 336 (1 drop, ca. 80 mg) and tetrakis(triphenylphosphine)palladium(0) (10 mg) were added in the sequence listed here. The reaction mixture was deaerated, immersed in an oil bath, and heated at reflux for 3–6 h. The molecular weight characteristics of the formed product were controlled every 30 min. The reaction was intentionally terminated when the weight average molecular weight M_w reached roughly 190 kg mol^{-1}. 4,4,5,5-Tetramethyl-2-phenyl-1,3,2-dioxaborolane (4.0 mg, 0.019 mmol) was added, and the reaction mixture was heated for additional 25 min. Afterwards, an excess of bromobenzene (300 mg, 1.9 mmol) was introduced and the mixture was stirred at reflux for another 25 min. Then, the mixture was cooled to room temperature, the polymer was extracted using 500 mL toluene; the resulting solution was washed three times with deionized water (250 mL), dried, and concentrated in vacuum (rotary evaporator) to 40 mL. Addition of 150 mL methanol precipitated the crude polymer. Subsequent purification was achieved using several additional dissolving/precipitation cycles. Finally, the precipitated polymer flakes were filtered into a cellulose thimble and processed by performing Soxhlet extraction using hexanes (12 h), acetone (12 h), dichloromethane (12 h), chloroform (8 h), and chlorobenzene (12 h). Very minor amount of the polymer remained undissolved as a residue in the thimble. The chlorobenzene extract was concentrated in vacuum to the volume of circa 20 mL, diluted with 20 mL 1,2-dichlorobenzene; and precipitated in methanol. The obtained dark green (almost black) solid was collected by filtration and dried in vacuum. The total yield of the purified polymer P2 ($M_w \approx 203$ kg mol^{-1}, PDI ≈ 4.6) was 79%.

Device preparation and characterization

The organic solar cells were fabricated on indium tin oxide (ITO) prepatterned glass substrates (Psiotec, UK) using a normal device architecture. First, a 50 nm hole-transporting layer of PEDOT:PSS (Clevios PH from HC Starck, Germany; 1:3.2 by volume with isopropanol) was deposited using a doctor blade (Erichsen, Germany) at 50 °C and 35 mm s^{-1} blade speed. In flexible devices, the same PEDOT:PSS ink was deposited on ITO prepatterened PET substrates using a slot-die coater[28] (Mini Roll Coater from FOM Technologies, Denmark) at 70 °C, a drum speed of 0.8 m min^{-1} and 0.30 mL min^{-1} ink flow. The coated substrates were then annealed at 140 °C for 20 min in air. For the reference spin-coated devices under inert conditions, the samples were transferred to a N_2-filled glovebox immediately after annealing. The active layer consisted of a blend of a low-bandgap polymer and $PC_{70}BM$ (Solenne BV, The Netherlands), which were deposited in all cases from a solution based on

o-dichlorobenzene (Aldrich, USA). The reference PCDTBT was obtained from 1-Material, Canada. Except for polymer P1 (1:1.2), the polymer-to-fullerene ratio was set to 1:2 and the total solution concentration varied from 15 to 20 mg mL^{-1}. For the new polymers, 0.625 vol% (for P1) or 0.312 vol% (for P2 and P3) of 1,8-diiodooctane (Aldrich) was added to the solution. The resulting solutions were filtered through a 0.45 μm pore size paper filter and then deposited on ITO/PEDOT:PSS substrates using one of the following techniques: a) spin-coating at 800–1100 rpm for 150 s; b) doctor-blade coating at 95 °C and 10–15 mm s^{-1}; c) slot-die coating at 70 °C, 0.2–0.3 m min^{-1}, and 0.02 mL min^{-1}; and d) inkjet printing (Fujifilm Dimatix, USA) as described in previous work.[21] The samples were then transferred to a N_2-filled glovebox where a second annealing step at 90 °C for 10 min was performed on samples based on P1, P2, and P3 (not on PCDTBT). The top cathode was deposited by sequential thermal evaporation (Angstrom Engineering, Canada) of Ca (20 nm at a rate of 0.2 Å s^{-1}) and Al (100 nm at 2 Å s^{-1}) at a base pressure of 10^{-6} mbar through a shadow mask, defining an active area of 9 mm^2 or 0.7 cm^2. Finally, the finished devices were encapsulated under a cover glass (Ossila, UK) using UV-activated adhesive (Ossila, UK).

The *J–V* characteristics of the solar cells were measured under AM 1.5G (Air Mass 1.5 Global) illumination using a solar simulator (Newport, USA) calibrated to 100 mW cm^{-2} light intensity and a source meter (Keithley, USA) under ambient conditions. External quantum efficiency (EQE) measurements were performed on a setup comprising a monochromated light source originating from a Xe lamp, a mechanical chopper, a preamplifier, and a lock-in amplifier (Newport Oriel, USA). Photocurrent maps were obtained using a PCT photoelectric test system (Botest, Germany) equipped with a 405 nm laser operated at 20% light intensity, 0 V constant bias voltage, and with both spot and step sizes set at 40 μm.

Acknowledgements

This work was co-funded by the European Regional Development Fund and the Republic of Cyprus through the Research Promotion Foundation (Strategic Infrastructure Project New Infrastructure/Strategic/0308/06). The synthesis of conjugated polymers P1–P3 used in this work was performed in the frame of the Russian Science Foundation project No. 14-13-01031.

Keywords: copolymers · photovoltaics · solar cells · solution processing · upscaling

[1] A. Facchetti, *Chem. Mater.* **2011**, *23*, 733.
[2] a) M. C. Scharber, D. Mühlbacher, M. Koppe, P. Denk, C. Waldauf, A. J. Heeger, C. J. Brabec, *Adv. Mater.* **2006**, *18*, 789; b) M. C. Scharber, N. S. Sariciftci, *Prog. Polym. Sci.* **2013**, *38*, 1929.
[3] G. Yu, J. Gao, J. C. Hummelen, F. Wudl, A. J. Heeger, *Science* **1995**, *270*, 1789.
[4] Y. Lin, Y. Li, X. Zhan, *Chem. Soc. Rev.* **2012**, *41*, 4245.
[5] H. Zhou, L. Yang, W. You, *Macromolecules* **2012**, *45*, 607.
[6] a) J. H. Park, E. H. Jung, J. W. Jung, W. H. Jo, *Adv. Mater.* **2013**, *25*, 2583; b) H. Chen, Y. Guo, G. Yu, Y. Zhao, J. Zhang, D. Gao, H. Liu, Y. Liu, *Adv. Mater.* **2012**, *24*, 4618; c) G. W. P. van Pruissen, E. A. Pidko, M. M. Wienk, R. A. J. Janssen, *J. Mater. Chem. C* **2014**, *2*, 731; d) L. Biniek, B. C. Schroeder, C. B. Nielsen, I. McCulloch, *J. Mater. Chem.* **2012**, *22*, 14803.
[7] a) H. K. H. Lee, Z. Li, I. Constantinou, F. So, S. W. Tsang, S. K. So, *Adv. Energy Mater.* **2014**, *4*, 1400768; b) N. Gasparini, A. Katsouras, M. I. Prodromidis, A. Avgeropoulos, D. Baran, M. Salvador, S. Fladischer, E. Spiecker, C. L. Chochos, T. Ameri, C. J. Brabec, *Adv. Funct. Mater.* **2015**, *25*, 4898.
[8] a) R. Søndergaard, M. Helgesen, M. Jørgensen, F. C. Krebs, *Adv. Energy Mater.* **2011**, *1*, 68; b) E. Wang, J. Bergqvist, K. Vandewal, Z. Ma, L. Hou, A. Lundin, S. Himmelberger, A. Salleo, C. Müller, O. Inganäs, F. Zhang, M. R. Andersson, *Adv. Energy Mater.* **2013**, *3*, 806; c) T. R. Andersen, T. T. Larsen-Olsen, B. Andreasen, A. P. L. Böttiger, J. E. Carlé, M. Helgesen, E. Bundgaard, K. Norrman, J. W. Andreasen, M. Jørgensen, F. C. Krebs, *ACS Nano* **2011**, *5*, 4188; d) P. Troshin, H. Hoppe, J. Renz, M. Egginger, J. Mayorova, A. E. Goryochev, A. Peregudov, R. Lyubovskaya, G. Gobsch, N. S. Sariciftci, V. Razumov, *Adv. Funct. Mater.* **2009**, *19*, 779.
[9] I. Kang, H. Yun, D. S. Chung, S. Kwon, Y. Kim, *J. Am. Chem. Soc.* **2013**, *135*, 14896.
[10] a) Y. W. Soon, H. Cho, J. Low, H. Bronstein, I. McCulloch, J. R. Durrant, *Chem. Commun.* **2013**, *49*, 1291; b) L. A. Frolova, N. P. Piven, D. K. Susarova, A. V. Akkuratov, S. D. Babenko, P. A. Troshin, *Chem. Commun.* **2015**, *51*, 2242.
[11] N. Blouin, A. Michaud, M. Leclerc, *Adv. Mater.* **2007**, *19*, 2295.
[12] C. H. Peters, I. T. Sachs-Quintana, J. P. Kastrop, S. Beaupré, M. Leclerc, M. D. McGehee, *Adv. Energy Mater.* **2011**, *1*, 491.
[13] T. Wang, N. W. Scarratt, H. Yi, A. D. F. Dunbar, A. J. Pearson, D. C. Watters, T. S. Glen, A. C. Brook, J. Kingsley, A. R. Buckley, M. W. A. Skoda, A. M. Donald, R. A. L. Jones, A. Iraqi, D. G. Lidzey, *Adv. Energy Mater.* **2013**, *3*, 505.
[14] a) L. Lucera, P. Kubis, F. W. Fecher, C. Bronnbauer, M. Turbiez, K. Forberich, T. Ameri, H. Egelhaaf, C. J. Brabec, *Energy Technol.* **2015**, *3*, 373 – 384; b) R. R. Søndergaard, M. Hösel, F. C. Krebs, *J. Polym. Sci. Part B* **2013**, *51*, 16; c) J. J. van Franeker, W. P. Voorthuijzen, H. Gorter, K. H. Hendriks, R. A. J. Janssen, A. Hadipour, R. Andriessen, Y. Galagan, *Sol. Energy Mater. Sol. Cells* **2013**, *117*, 267; d) D. Kaduwal, H.-F. Schleiermacher, J. Schulz-Gericke, S. Schiefer, Y. Liang Tan, J. Zhang, B. Zimmermann, U. Würfel, *Sol. Energy Mater. Sol. Cells* **2015**, *136*, 200; e) D. Vak, K. Hwang, A. Faulks, Y.-S. Jung, N. Clark, D.-Y. Kim, G. J. Wilson, S. E. Watkins, *Adv. Energy Mater.* **2015**, *5*, DOI: 10.1002/aenm.201401539; f) I. Burgués-Ceballos, M. Stella, P. D. Lacharmoise, E. Martinez-Ferrero, *J. Mater. Chem. A* **2014**, *2*, 17711; g) S. Hong, J. Lee, H. Kang, K. Lee, *Sol. Energy Mater. Sol. Cells* **2013**, *112*, 27; h) H. Youn, H. J. Park, L. J. Guo, *Small* **2015**, *11*, 2228.
[15] a) A. V. Akkuratov, D. K. Susarova, O. V. Kozlov, A. V. Chernyak, Y. L. Moskvin, L. A. Frolova, M. S. Pshenichnikov, P. A. Troshin, *Macromolecules* **2015**, *48*, 2013; b) I. E. Kuznetsov, A. V. Akkuratov, D. K. Susarova, D. V. Anokhin, Y. L. Moskvin, M. V. Kluyev, P. A. Troshin, *Chem. Commun.* **2015**, *51*, 7562; c) A. V. Akkuratov, D. K. Susarova, D. V. Novikov, D. V. Anokhin, Y. L. Moskvin, A. V. Chernyak, F. A. Prudnov, S. D. Babenko, P. A. Troshin, *J. Mater. Chem. C* **2015**, *3*, 1497.
[16] a) T. Wang, A. J. Pearson, A. D. F. Dunbar, P. A. Staniec, D. C. Watters, H. Yi, A. J. Ryan, R. A. L. Jones, A. Iraqi, D. G. Lidzey, *Adv. Funct. Mater.* **2012**, *22*, 1399; b) S. Alem, T.-Y. Chu, S. C. Tse, S. Wakim, J. Lu, R. Movileanu, Y. Tao, F. Bélanger, D. Désilets, S. Beaupré, M. Leclerc, S. Rodman, D. Waller, R. Gaudiana, *Org. Electron.* **2011**, *12*, 1788.
[17] a) S. H. Park, A. Roy, S. Beaupré, S. Cho, N. Coates, J. S. Moon, D. Moses, M. Leclerc, K. Lee, A. J. Heeger, *Nat. Photonics* **2009**, *3*, 297; b) K. X. Steirer, P. F. Ndione, N. E. Widjonarko, M. T. Lloyd, J. Meyer, E. L. Ratcliff, A. Kahn, N. R. Armstrong, C. J. Curtis, D. S. Ginley, J. J. Berry, D. C. Olson, *Adv. Energy Mater.* **2011**, *1*, 813; c) K.-G. Lim, M.-R. Choi, H.-B. Kim, J. H. Park, T.-W. Lee, *J. Mater. Chem.* **2012**, *22*, 25148; d) Y. Zhang, H. Zhou, J. Seifter, L. Ying, A. Mikhailovsky, A. J. Heeger, G. C. Bazan, T.-Q. Nguyen, *Adv. Mater.* **2013**, *25*, 7038.
[18] E. Bovill, H. Yi, A. Iraqi, D. G. Lidzey, *Appl. Phys. Lett.* **2014**, *105*, 223302.
[19] Z. Li, C. R. McNeill, *J. Appl. Phys.* **2011**, *109*, 074513.
[20] C. N. Hoth, S. A. Choulis, P. Schilinsky, C. J. Brabec, *Adv. Mater.* **2007**, *19*, 3973.
[21] F. Hermerschmidt, P. Papagiorgis, A. Savva, C. Christodoulou, G. Itskos, S. A. Choulis, *Sol. Energy Mater. Sol. Cells* **2014**, *130*, 474.
[22] a) C. N. Hoth, P. Schilinsky, S. A. Choulis, C. J. Brabec, *Nano Lett.* **2008**, *8*, 2806; b) M. Koppe, C. J. Brabec, S. Heiml, A. Schausberger, W. Duffy, M. Heeney, I. McCulloch, *Macromolecules* **2009**, *42*, 4661.
[23] A. Teichler, J. Perelaer, U. S. Schubert, *J. Mater. Chem. C* **2013**, *1*, 1910.
[24] C. Lungenschmied, G. Dennler, H. Neugebauer, S. N. Sariciftci, M. Glatthaar, T. Meyer, A. Meyer, *Sol. Energy Mater. Sol. Cells* **2007**, *91*, 379.

[25] Y. Galagan, E. W. C. Coenen, B. Zimmermann, L. H. Slooff, W. J. H. Verhees, S. C. Veenstra, J. M. Kroon, M. Jørgensen, F. C. Krebs, R. Andriessen, *Adv. Energy Mater.* **2014**, *4*, 1300498.

[26] a) Z. M. Beiley, E. T. Hoke, R. Noriega, J. Dacuña, G. F. Burkhard, J. A. Bartelt, A. Salleo, M. F. Toney, M. D. McGehee, *Adv. Energy Mater.* **2011**, *1*, 954; b) T. M. Clarke, J. Peet, A. Nattestad, N. Drolet, G. Dennler, C. Lungenschmied, M. Leclerc, A. J. Mozer, *Org. Electron.* **2012**, *13*, 2639; c) J. S. Moon, J. Jo, A. J. Heeger, *Adv. Energy Mater.* **2012**, *2*, 304.

[27] a) H. F. Dam, F. C. Krebs, *Sol. Energy Mater. Sol. Cells* **2012**, *97*, 191; b) J. E. Carlé, T. R. Andersen, M. Helgesen, E. Bundgaard, M. Jorgensen, F. C. Krebs, *Sol. Energy Mater. Sol. Cells* **2013**, *108*, 126.

[28] S. A. Gevorgyan, J. E. Carlé, R. Søndergaard, T. T. Larsen-Olsen, M. Jørgensen, F. C. Krebs, *Sol. Energy Mater. Sol. Cells* **2013**, *110*, 24.

Received: August 20, 2015
Revised: October 16, 2015
Published online on ■■ ▮▮, 0000

I. Burgués-Ceballos, F. Hermerschmidt, A. V. Akkuratov, D. K. Susarova, P. A. Troshin, S. A. Choulis*

■■ – ■■

High-Performing Polycarbazole Derivatives for Efficient Solution-Processing of Organic Solar Cells in Air

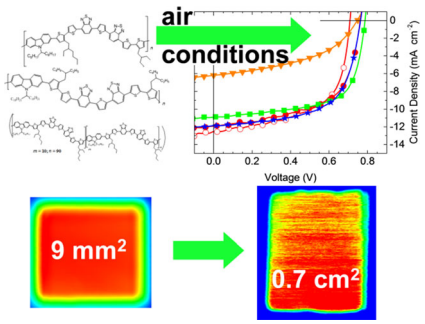

Fabricate them in air: A series of poly(2,7-carbazole) derivatives are used to fabricate organic solar cells in air using roll-to-roll-compatible deposition methods. High efficiencies are obtained both in rigid and in flexible devices. Initial defects in photocurrent generation are identified when moving from millimeter-sized to centimeter-sized devices.